J. Fluid Mech. (2001), *vol.* 444, *pp.* 175–198. Printed in the United Kingdom

Exact solutions for steady bubbles in a Hele-Shaw cell with rectangular geometry

By GIOVANI L. VASCONCELOS

Laboratório de Física Teórica e Computacional, Departamento de Física,
Universidade Federal de Pernambuco, 50670-901, Recife, Brazil

(Received 16 June 2000 and in revised form 18 April 2001)

Exact solutions are presented for an arbitrary number of steadily moving bubbles in a Hele-Shaw channel when surface tension is neglected. According to the symmetry displayed by the bubbles, the solutions are classified into two groups: (i) solutions where the bubbles are symmetrical about the channel centreline and (ii) solutions in which the bubbles have fore-and-aft symmetry. The general solutions are expressed in integral form but in some special cases analytic solutions in terms of elliptic integrals are found. The possible relevance of these exact solutions to experiments is also briefly discussed.

1. Introduction

The motion of the interface between two viscous fluids in a Hele-Shaw cell, where the fluids are confined between two closely spaced flat plates, has attracted considerable attention in the last twenty years and there is now a rather large body of literature on the subject.† A great deal of this research has been motivated, in part, by the mathematical analogies between the Hele-Shaw system and other important moving-boundary problems, such as dendritic crystal growth and direct solidification (see, for example, Pelcé 1988). Because it is a system where controlled experiments are relatively easy to perform and which is also amenable to mathematical investigation, the Hele-Shaw cell has become the 'laboratory' of choice to study the dynamics of interfaces between two viscous fluids.

From a theoretical standpoint, the problem of interfacial dynamics in a Hele-Shaw cell is particularly tractable when surface tension effects are neglected, and several exact solutions have been found in this case for both steady and time-dependent flows. Exact solutions for the problem were first obtained by Saffman & Taylor (1958) for a steadily moving finger, and subsequently Taylor & Saffman (1959) found solutions for a single symmetrical bubble as well as for an asymmetrical finger. The single bubble solution was later extended by Tanveer (1987) to include non-symmetric bubbles. Exact solutions for a stream of bubbles have been reported by Burgess & Tanveer (1991). An exact solution for a non-symmetric finger in a Hele-Shaw cell tilted sideways has also been obtained by Brener, Levine & Tu (1991). A rotation invariance for steady Hele-Shaw flows has recently been discovered by Vasconcelos (1993*a*) and Tian & Vasconcelos (1993). This property was then used by the present author to obtain several new exact solutions, such as a periodic solution with an arbitrary number of bubbles per unit cell (Vasconcelos 1994) and solutions for multiple fingers

† A comprehensive bibliography on Hele-Shaw flows up to 1998 can be found at http://maths.ox.ac.uk/∼howison/Hele-Shaw.

(Vasconcelos 1998, 2001) as well as for a finger with an arbitrary number of bubbles ahead of the finger tip (Vasconcelos 1999). More recently, a preliminary description of an analytic solution in terms of elliptic integrals for two bubbles and for a finger with a bubble at the tip has also been given by Vasconcelos (2000).

Time-dependent solutions also date back to early work by Saffman (1959) and since then many other solutions in the form of the so-called 'pole dynamics' have been found (see for example Howison 1992 for a review). Most of these time-dependent solutions with zero surface tension develop a cusp in finite time but recently Dawson & Mineev-Weinstein (1994) and Baker, Siegel & Tanveer (1995) have studied a class of solutions that remain regular for all times and that asymptotically approach the multifinger solution mentioned above. Self-similar solutions for an expanding finger in a wedge geometry have also been obtained by Ben Amar (1991*a*, *b*).

For non-zero surface tension, on the other hand, the problem becomes quite hard to tackle analytically and there is so far only one non-trivial exact solution (Vasconcelos & Kadanoff 1991; Vasconcelos 1993*b*), which is mainly of academic interest for it involves somewhat extraneous boundary conditions. Notwithstanding this difficulty, the effect of a small amount of surface tension has been extensively studied in connection with the so-called selection problem. This problem refers to the fact that exact solutions at zero surface tension are usually degenerate in the sense that fixing the physical parameters of the solution (e.g. the bubble size) does not determine the interface velocity. The selection problem was first noted by Saffman & Taylor (1958) who found in their experiments that the finger with relative width $\lambda = 1/2$ was selected out of the one-parameter family of analytic solutions with zero surface tension. This problem is now fairly well understood theoretically: asymptotics beyond all orders predicts that for a given value of surface tension λ has a discrete set of values, all of which converge to $\lambda = 1/2$ as surface tension approaches zero; for reviews, see e.g. Kessler, Koplik & Levine (1988), Pelcé (1988) and Tanveer (1992). A similar solvability analysis has been carried out, for example, in the case of a single bubble (Tanveer 1986). An alternative selection theory for the Saffman–Taylor finger based solely on zero surface tension solutions has recently been proposed by Mineev-Weinstein (1998).

The problem of a finger with a small bubble at the tip has also been studied experimentally by Couder, Gérard & Rabaud (1986) and Rabaud, Couder & Gérard (1988). Here it was found that owing to the presence of the bubble the finger was considerably narrower than the usual Saffman–Taylor finger. A similar effect has been observed for bubbles: when a small bubble attaches to the nose of a larger bubble, the larger bubble becomes more elongated and its velocity increases (Ikeda & Maxworthy 1990). This narrowing effect induced by the small bubble has not yet been completely understood. Hong & Langer (1987) and Hong & Family (1988) have proposed an approximate selection theory for a finger with a small bubble at the tip and for a large bubble with a small one at the the nose, respectively. This theory, which is based on the solutions for a pure finger and a single bubble at zero surface tension, is somewhat unsatisfactory in that the effect of the small bubble is taken into account through a rather unphysical condition, namely, a cusp at the leading front of the perturbed interface. A more detailed (but still approximate) analysis of the selection problem for a finger with a bubble was performed by Combescot & Dombre (1989). These authors computed an approximate solution at zero surface tension for the case of a small bubble far ahead of the finger, and then showed that in the limit of vanishingly small surface tension fingers with $\lambda < 1/2$ were possible.

In the present paper, we report new exact solutions for an arbitrary number N

of bubbles moving with a constant velocity in a Hele-Shaw channel when surface tension is neglected. According to their symmetry, these solutions are divided into two classes: (i) solutions where the bubbles are symmetric about the channel centreline and (ii) solutions in which the bubbles have fore-and-aft symmetry. Our solutions are constructed using conformal mappings and here again use is made of the rotation invariance displayed by steady Hele-Shaw flows. The general solutions are expressed in integral form but we anticipate that analytic solutions in terms of elliptic integrals are found in some special cases that include a single asymmetrical bubble and a pair of centreline-symmetric bubbles.

We emphasize here that although the solutions reported in the present paper are for the idealized case of zero surface tension they are nevertheless of practical relevance. For example, some of the many-bubble solutions described below resemble actual shapes observed by Maxworthy (1986) in his experiment on rising bubbles in a Hele-Shaw cell. Furthermore, our two-bubble solution has been shown (Vasconcelos 2000) to be in good agreement with shapes observed in the experiments conducted by Ikeda & Maxworthy (1990) on the motion of a large bubble with a small one attached to its nose. Moreover, exact solutions at zero surface tension are of great importance in connection with the selection problem discussed above. For example, a more rigorous solvability analysis for two bubbles (as well as for a finger with a bubble) could in principle be carried out having as starting point our family of analytic solutions for this case. In spite of the great interest in this selection problem, issues concerning the effect of surface tension are however beyond the scope of the present paper.

The paper is organized as follows. In § 2 the problem for N steady bubbles in a Hele-Shaw channel with zero surface tension is mathematically formulated. In § 3 we present our exact solutions for the case where the bubbles are symmetrical about the channel centreline. In particular, we obtain in § 3.3 an analytic solution in terms of elliptic integrals for the case of two unequal bubbles in a Hele-Shaw cell. In § 4 we discuss the case in which the bubbles have fore-and-aft symmetry. Here we also find an exact solution for a single bubble in terms of elliptic integrals. Our conclusions and main results are summarized in § 5.

2. Mathematical formulation

2.1. *Equations of motion*

We consider the problem of N bubbles moving with a constant velocity U in the x-direction in a rectangular Hele-Shaw cell of width $2a$, where the fluid velocity at infinity is equal to V. In order to render the problem analytically tractable we shall adopt, as usual, some simplifying assumptions. First, we will assume that the fluid inside the bubbles (say, air) has negligible viscosity so that the pressure inside a bubble will be taken as constant. Secondly, surface tension will be neglected and hence the viscous-fluid pressure will have a constant value along the bubble surface. Thirdly, we shall neglect three-dimensional effects due to the thin film between the bubbles and the plates. Fourthly, we will assume that the cell is horizontally placed so that gravity plays no rôle. (The case of a cell tilted upward, as used, for example, in the experiments by Maxworthy (1986) and Ikeda & Maxworthy (1990), can be transformed into a horizontal setup by a suitable change of variables; see Saffman & Taylor (1958) for details.) Finally, we shall concern ourselves here with situations where the bubbles display either one of the following two symmetries: (i) symmetry

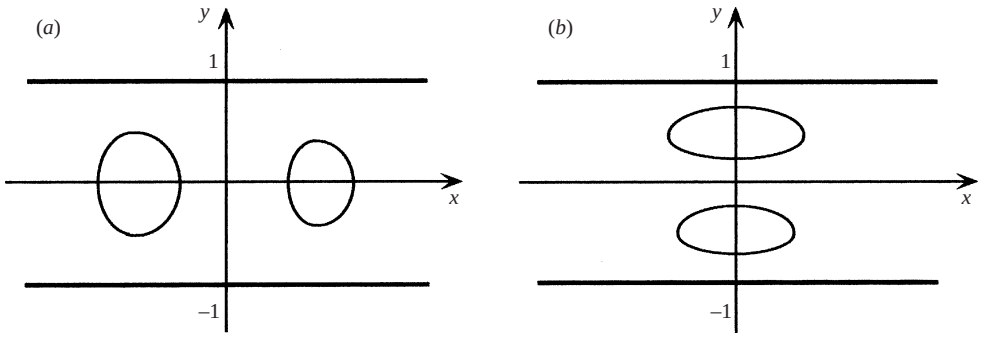

FIGURE 1. Multiple bubbles in a Hele-Shaw channel: (*a*) bubbles with centreline symmetry and (*b*) bubbles with fore-and-aft symmetry.

about the channel centreline (figure 1*a*) or (ii) fore-and-aft symmetry, that is, symmetry about an axis perpendicular to the centreline (figure 1*b*).

The velocity $\boldsymbol{v}(x, y)$, averaged across the gap, for a viscous fluid in a Hele-Shaw cell is governed by the equations

$$\boldsymbol{v} = \nabla\phi, \tag{2.1}$$

$$\nabla \cdot \boldsymbol{v} = \nabla^2\phi = 0, \tag{2.2}$$

where the velocity potential $\phi(x, y)$ is given by

$$\phi = -\frac{b^2}{12\mu}p. \tag{2.3}$$

Here b is the gap between the cell plates, μ is the viscosity, and p is the fluid pressure.

Let us now denote by $\mathscr{C}_k$ the interface corresponding to the kth bubble, where $k = 1, 2, \ldots, N$, and take the channel walls to be at $y = \pm a$. In order to define the problem completely we need to specify the boundary conditions to be satisfied by the velocity potential $\phi(x, y)$ on $\mathscr{C}_k$, at $y = \pm a$, and at infinity. Here, however, it is more convenient to work in a reference frame moving with the bubbles and introduce dimensionless quantities. Following Saffman & Taylor (1958), we thus consider dimensionless variables defined by

$$x' = (x - Ut)/a, \quad y' = y/a, \tag{2.4}$$

$$\phi' = \frac{\phi - Ux}{(U - V)a}, \quad \psi' = \frac{\psi - Uy}{(U - V)a}, \tag{2.5}$$

where $\psi(x, y)$ is the associated stream function. We now have that ϕ' and ψ' must satisfy the conditions

$$\psi' = \mp 1 \quad \text{on} \quad y' = \pm 1, \tag{2.6}$$

$$\psi' = \psi'_k \quad \text{and} \quad \phi' = -\mathscr{U}x' + \phi'_k \quad \text{on} \quad \mathscr{C}_k, \tag{2.7}$$

$$\phi' \approx -x' \quad \text{and} \quad \psi' \approx -y' \quad \text{as} \quad |x'| \to \infty, \tag{2.8}$$

where ψ'_k and ϕ'_k are constants to be specified later and the dimensionless bubble velocity $\mathscr{U}$ is given by

$$\mathscr{U} = U/(U - V). \tag{2.9}$$

The physical meaning of the conditions above should be evident: (2.6) is the condition that the walls be streamlines of the flow; the first condition in (2.7) says that the

interfaces $\mathscr{C}_k$ when viewed in the moving frame are also streamlines, while the second condition in (2.7) states that the pressure p and hence ϕ is constant along $\mathscr{C}_k$; and finally (2.8) is merely a restatement of the fact that at infinity the fluid has a constant velocity V in the lab frame and thus a dimensionless unity velocity in the moving frame. Henceforth we shall drop the prime notation with the understanding that we shall be working in the reference frame moving with the bubbles and using dimensionless quantities, unless noted otherwise.

As is well known, the problem of potential flows in two dimensions can be also formulated in terms of the complex potential $W(z) = \phi + \mathrm{i}\psi$, where $z = x + \mathrm{i}y$. The function $W(z)$ must then be analytic in the viscous-fluid region and satisfy the appropriate boundary conditions:

$$\operatorname{Im} W = \mp 1 \quad \text{on} \quad y = \pm 1, \tag{2.10}$$

$$W = -\mathscr{U}x + \phi_k + \mathrm{i}\psi_k \quad \text{on} \quad \mathscr{C}_k, k = 1, \ldots, N, \tag{2.11}$$

$$W \approx -z \quad \text{as} \quad |x| \to \infty, \tag{2.12}$$

as follows from (2.6)–(2.8). Here $\operatorname{Im} W$ denotes the imaginary part of W.

The complex potential $W(z)$ can alternatively be seen as a conformal mapping from the fluid region in the z-plane onto the corresponding flow domain in the W-plane. Now, the existence of either one of the two symmetries mentioned above simplifies considerably the problem because the relevant flow domains can be reduced to simply connected regions. For instance, in the case of centreline symmetry one needs to consider the problem only in one half, say the upper half, of the original channel, as indicated in figure 2(*a*). In this case we have $\psi_k = 0$ for all k, since the bubbles all lie on the same streamline $\psi = 0$, and $\phi_k < \phi_j$ for $k > j$, reflecting the fact the bubbles farther upstream are at higher pressures. The corresponding flow domain in the W-plane for this symmetry is shown in figure 2(*b*). Similarly, in the case of fore-and-aft symmetry one can reduce the problem to the right-hand side of the channel, as indicated in figure 3(*a*). Now $\phi_k = 0$ for all k, since the bubbles are at the same pressure, which we take to be zero, and the ψ_k are all different for the bubbles lie on different streamlines. The respective domain in the W-plane is shown in figure 3(*b*).

2.2. *The rotated problem*

An interesting rotation invariance for steady Hele-Shaw flows has recently been discovered by Tian & Vasconcelos (1993). These authors showed that if a curve $\mathscr{C}$ is a solution for a bubble moving with constant velocity U in the x-direction in an unbounded Hele-Shaw cell, then the curve $\tilde{\mathscr{C}}$ obtained from a rotation of $\mathscr{C}$ about the origin by an angle α is also a solution with the same velocity U. In the present paper we shall make use of their result to construct exact solutions for N steady bubbles in a Hele-Shaw channel. Here however we will adopt a viewpoint slightly different from that originally used by Tian & Vasconcelos (1993). More specifically, we will view the new rotated solution as one in which the bubble itself was kept fixed while its velocity has been rotated by an angle α. In order to make the paper self-contained we shall quote below the main result of Tian & Vasconcelos (1993), albeit in a slightly modified form to accord with our viewpoint. The interested reader is referred to their original paper for details of the proof. (For ease of comparison with their results, we shall use dimensional variables in the next paragraph but will afterward return to our dimensionless quantities.)

Suppose that $W(z)$ is the complex potential (in the moving frame) for the problem of a bubble $\mathscr{C}$ moving with a constant velocity $\boldsymbol{U} = (U, 0)$ in an unbounded Hele-

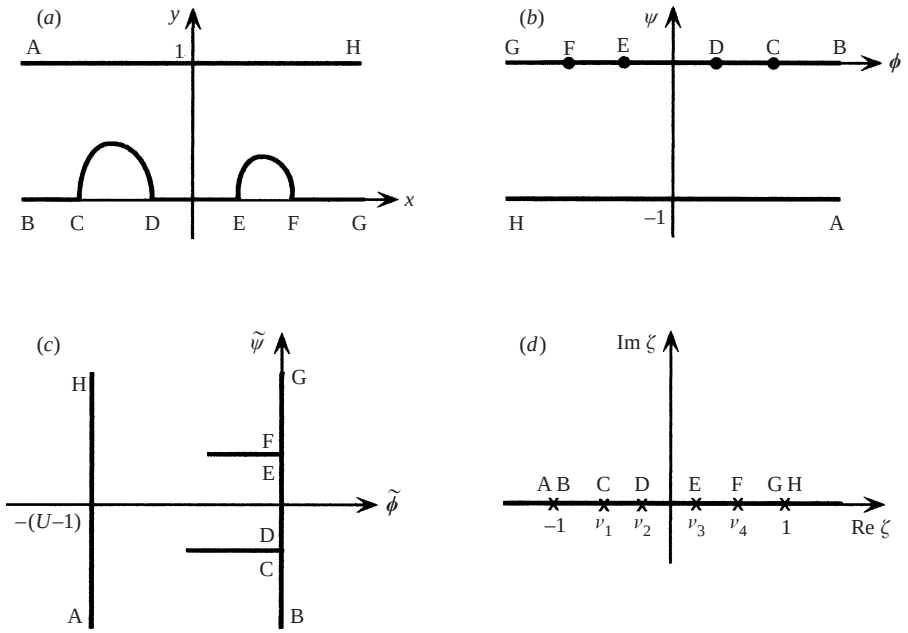

FIGURE 2. The flow geometry for bubbles with centreline symmetry: (*a*) the z-plane, (*b*) the W-plane, (*c*) the $\tilde{W}$-plane, and (*d*) the upper half-ζ-plane.

Shaw flow where the fluid has a uniform velocity $\boldsymbol{V} = (V, 0)$ at infinity and surface tension has been neglected. Then the complex potential

$$\tilde{W}(z) = \mathrm{e}^{\mathrm{i}\alpha} W(z) + \mathrm{i}U \sin\alpha\, z \tag{2.13}$$

is also a solution for a Hele-Shaw flow where the bubble $\mathscr{C}$ moves with the same speed U but now in a direction making an angle α with the original velocity, that is, the new bubble velocity $\boldsymbol{U}'$ is given by

$$\boldsymbol{U}' = (U\cos\alpha, U\sin\alpha), \tag{2.14}$$

whereas the fluid velocity $\boldsymbol{V}'$ at infinity is

$$\boldsymbol{V}' = (V\cos\alpha, (U - V)\sin\alpha). \tag{2.15}$$

Here $\tilde{W}(z)$ corresponds to the complex potential in the moving frame for the rotated problem. The result above holds in general so long as the original complex potential $W(z)$ is defined on (or can be extended to) an unbounded Hele-Shaw cell (Tian & Vasconcelos 1993). It therefore applies to steady bubbles in a Hele-Shaw channel, since in this case the complex potential $W(z)$ can be trivially extended to the entire z-plane by succesive Schwarz reflections.

Of special interest to us here is the solution corresponding to a rotation by 90°, where the bubbles move with the same velocity U as in the original solution but now in the y-direction. In this case the region occupied by the fluid in the rotated solution is exactly the same as that for the original problem, the main difference being that now the channel walls become equipotentials of the flow. Setting $\alpha = \pi/2$ in (2.13) we obtain for the rotated complex potential $\tilde{W}(z)$:

$$\tilde{W}(z) = \mathrm{i}[W(z) + \mathscr{U}z], \tag{2.16}$$

where we have switched back to dimensionless quantities. From (2.10)–(2.12) and

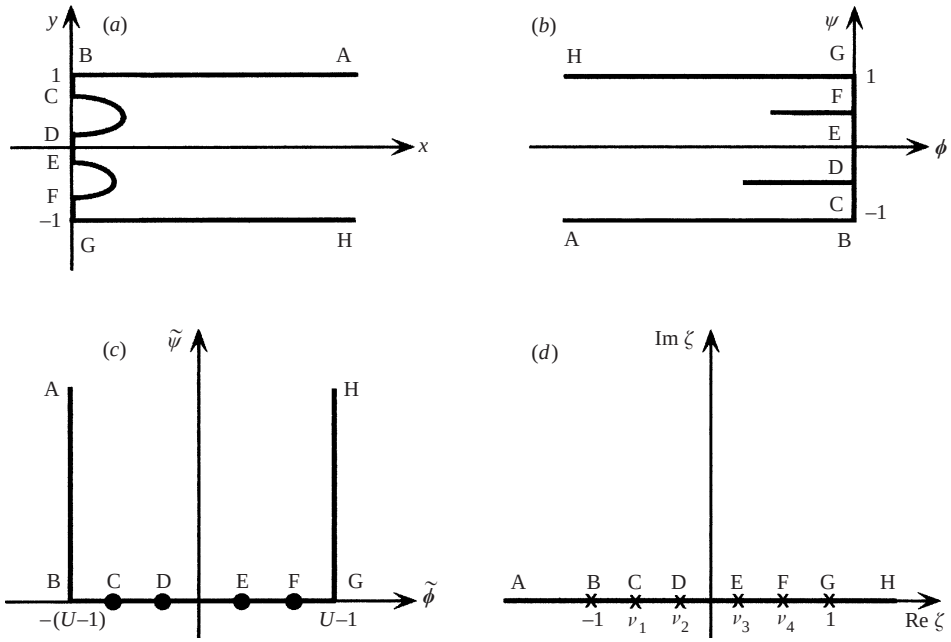

FIGURE 3. The flow geometry for bubbles with fore-and-aft symmetry: (*a*) the z-plane, (*b*) the W-plane, (*c*) the $\tilde{W}$-plane, and (*d*) the upper half-ζ-plane.

(2.16) it then follows that $\tilde{W}(z)$ satisfies the following boundary conditions:

$$\operatorname{Re}\tilde{W} = \mp(\mathscr{U}-1) \quad \text{on} \quad y = \pm 1, \tag{2.17}$$

$$\tilde{W} = -\mathscr{U}y - \psi_k + \mathrm{i}\phi_k \quad \text{on} \quad \mathscr{C}_k, \quad k = 0, 1, \ldots, N, \tag{2.18}$$

$$\tilde{W} \approx \mathrm{i}(\mathscr{U}-1)z \quad \text{as} \quad |x| \to \infty, \tag{2.19}$$

where $\operatorname{Re}\tilde{W}$ denotes the real part of $\tilde{W}$. In figures 2(*c*) and 3(*c*) we show the respective flow domains in the $\tilde{W}$-plane for the two symmetries under consideration in this paper.

2.3. *Conformal mapping formulation*

We now introduce a conformal mapping formulation that will allow us to construct exact solutions for the problem of N steady bubbles in a Hele-Shaw channel. At this stage, however, we shall present only the general aspects of the formalism that are valid for both symmetries considered in the present paper. Discussion of specific solutions for each symmetry will be deferred to the next sections.

First consider the conformal mapping $z = f(\zeta)$ from the upper half-ζ-plane onto the fluid domain in the z-plane; see figures 2(*d*) and 3(*d*). Here the two intervals $\operatorname{Re}\zeta = 0$, $|\zeta| > 1$ are mapped onto the channel walls, while the bubbles $\mathscr{C}_k$ are the image under $f(\zeta)$ of the intervals $\mathscr{I}_k$ on the real ζ axis defined by

$$\mathscr{I}_k \equiv (\nu_{2k-1}, \nu_{2k}), \quad k = 1, \ldots, N, \tag{2.20}$$

with $-1 < \nu_1 < \nu_2 < \ldots < \nu_{2N} < 1$. Now let $W = \Phi(\zeta)$ and $\tilde{W} = \Sigma(\zeta)$ be the conformal mappings from the upper half-ζ-plane onto the flow domains in the W- and $\tilde{W}$-planes, respectively. From (2.16) it then follows that the mapping function

$f(\zeta)$ can be written as

$$f(\zeta) = -\frac{1}{\mathscr{U}}[\Phi(\zeta) + \mathrm{i}\Sigma(\zeta)]. \tag{2.21}$$

From this equation and the fact that both $\Phi(\zeta)$ and $\Sigma(\zeta)$ have constant imaginary parts for $\zeta = s \in \mathscr{I}_k$, it then follows that the bubble $\mathscr{C}_k$ is given by the following parametric equations:

$$x_k(s) = \frac{1}{\mathscr{U}}[\phi_k - \mathrm{Re}\,\Phi(s)], \tag{2.22}$$

$$y_k(s) = -\frac{1}{\mathscr{U}}[\psi_k + \mathrm{Re}\,\Sigma(s)], \tag{2.23}$$

where ψ_k and ϕ_k are the imaginary parts of $\Phi(s)$ and $\Sigma(s)$ for $s \in \mathscr{I}_k$, respectively. (Recall that $\psi_k = 0$ for centreline symmetry, whereas $\phi_k = 0$ in the case of fore-and-aft symmetry.)

Summarizing our procedure so far, we have reduced our original free-boundary problem to the much simpler problem of obtaining two conformal mappings, namely, $W = \Phi(\zeta)$ and $\tilde{W} = \Sigma(\zeta)$, from the upper half-$\zeta$-plane onto respective *rectangular* domains in the W- and $\tilde{W}$-planes. As we will see shortly, such mappings can be easily obtained from the Schwarz–Christoffel formula (Carrier, Krook & Pearson 1983). It should also be noted that in previous solutions that use conformal mapping (see e.g. Tanveer 1987), once the mapping $W = \Phi(\zeta)$ from the chosen domain in the ζ-plane to the flow domain in the W-plane is known, then the mapping $z = f(\zeta)$ is constructed explicitly so as to satisfy the appropriate boundary conditions. Our method has the advantage of making this step rather straighforward by identifying the function $\tilde{W}(z) = \mathrm{i}[W(z) + Uz]$ with the complex potential for the rotated problem, so that solving for the mapping $\tilde{W} = \Sigma(\zeta)$ then completes the solution. Before presenting our specific solutions, however, a few comments regarding the case $\mathscr{U} = 2$ are in order.

Solutions with $\mathscr{U} = 2$ are special in the sense that solutions for any $\mathscr{U} > 1$ can be generated by a proper rescaling of the former solutions. This property was first noted by Millar (1992) in the context of the Taylor–Saffman solution for a single bubble and later shown by Vasconcelos (1994) to hold for any number of steady bubbles in a Hele-Shaw channel. Since we shall make use of this property in what follows, it is desirable to outline its proof here. First, notice that the flow domain in the W-plane does not depend on the bubble velocity $\mathscr{U}$, see figures 2(*b*) and 3(*b*), and hence the mapping function $\Phi(\zeta)$ will have no dependence on $\mathscr{U}$. The mapping function $\Sigma(\zeta)$, on the other hand, does depend on $\mathscr{U}$ but in a somewhat trivial manner since the domain in the $\tilde{W}$-plane for arbitrary $\mathscr{U}$ can be obtained from a rescaling of the domain for $\mathscr{U} = 2$; see figures 2(*c*) and 3(*c*). We thus have

$$\Phi_{\mathscr{U}}(\zeta) = \Phi_2(\zeta), \tag{2.24}$$

$$\Sigma_{\mathscr{U}}(\zeta) = (\mathscr{U} - 1)\Sigma_2(\zeta), \tag{2.25}$$

where we have used subscripts to indicate explicitly the dependence on the velocity $\mathscr{U}$. Let us now denote by $z_k^0(s) = x_k^0(s) + \mathrm{i}y_k^0(s)$ the solution for the kth bubble with $\mathscr{U} = 2$ for a given set of parameters $\{v_i\}$. Using (2.24) and (2.25) in connection with (2.22) and (2.23), one readily finds that the solution $z_k(s) = x_k(s) + \mathrm{i}y_k(s)$ for the bubble $\mathscr{C}_k$ moving with velocity $\mathscr{U}$ can be written as

$$x_k(s) = \rho\phi_k^0 + (1 - \rho)x_k^0(s), \tag{2.26}$$

$$y_k(s) = \rho\psi_k + (1 + \rho)y_k^0(s), \tag{2.27}$$

where $\rho = 1 - 2/\mathscr{U}$ and $\phi_k^0 = [\phi_k]_{\mathscr{U}=2}$. This result thus shows that solutions for any $\mathscr{U} > 1$ can be obtained (up to a rigid translation) by a mere rescaling of the solution with $\mathscr{U} = 2$. For $1 < \mathscr{U} < 2$ (i.e. $U > 2V$) such a rescaling corresponds to an expansion of the x-coordinate and a contraction of the y-coordinate, while for $\mathscr{U} > 2$ (i.e. $V < U < 2V$) the reverse occurs. In view of this property, we shall consider only the case $\mathscr{U} = 2$ in the remainder of the paper.

3. Bubbles with centreline symmetry

In this section we present exact solutions for the case shown in figure 2 in which the bubbles are symmetrical about the channel centreline. As discussed in the preceding section, in order to construct exact solutions for the problem we need to obtain the corresponding conformal mappings $W = \Phi(\zeta)$ and $\tilde{W} = \Sigma(\zeta)$. In what follows, we will first give a general solution in integral form for an arbitrary number N of bubbles and then proceed to discuss the cases $N = 1$ and $N = 2$ for which there exist analytic solutions for the bubble shapes.

3.1. *General solution for multiple bubbles*

We begin by recalling that in the case of centreline symmetry the flow domain in the W-plane is simply the strip $-1 < \psi < 0$; see figure 2(*b*). The conformal mapping from the upper half-ζ-plane onto such a strip is effected by the function

$$\Phi(\zeta) = -\frac{2}{\pi} \tanh^{-1} \zeta, \tag{3.1}$$

where we have omitted for brevity an additive real-valued constant. (This constant is chosen so as to fix the zero of the velocity potential ϕ.) Now, in the $\tilde{W}$-plane the domain consists of the strip $-1 < \tilde{\phi} < 0$ with N horizontal slits, as seen in figure 2(*c*) for $\mathscr{U} = 2$. This domain can be viewed as a degenerate polygon and so the corresponding mapping $\tilde{W} = \Sigma(\zeta)$ can be obtained from the Schwarz–Christoffel formula (Carrier *et al.* 1983). One then finds

$$\Sigma(\zeta) = \Sigma_0 + \frac{\mathrm{i}C}{\pi} \int_{\zeta_0}^{\zeta} \frac{\prod_{j=1}^{N} (\zeta - \gamma_j)}{(\zeta^2 - 1) \prod_{j=1}^{2N} (\zeta - v_j)^{1/2}} \, \mathrm{d}\zeta, \tag{3.2}$$

where C is a real-valued constant and $\gamma_j \in \mathscr{I}_j$, with $\mathscr{I}_j$ as defined in (2.20). The initial point ζ_0 in (3.2) can be chosen arbitrarily and the constant Σ_0 is then adjusted to fix the origin in the $\tilde{W}$-plane. Here we have chosen to map $\zeta = \pm 1$ to $\tilde{W} = \pm\infty$, as shown in figure 2. In view of the third degree of freedom of Riemann's mapping theorem one could also fix the value of one given v_j. At this stage, it is best however to proceed with this 'degeneracy' and consider the v_j as $2N$ free parameters (even though only $2N - 1$ of them are actually independent).

For calculation purposes it is convenient to expand the numerator in (3.2) and so we write

$$\Sigma(\zeta) = \Sigma_0 + \frac{2\mathrm{i}}{\pi} \int_{\zeta_0}^{\zeta} \frac{\sum_{j=0}^{N} a_j \zeta^j}{(1 - \zeta^2) \prod_{j=1}^{2N} (\zeta - v_j)^{1/2}} \, \mathrm{d}\zeta, \tag{3.3}$$

where the a_j are real-valued coefficients. (The a_j could of course be expressed in terms of the γ_j but we will not present this detail here for we prefer to work directly with the mapping (3.3).) For a given set of parameters v_j the coefficients a_j are determined

as follows. First, let us define the quantities I_{jk}

$$I_{jk} = \int_{v_{2k-1}}^{v_{2k}} \frac{t^j}{(1-t^2)\prod_{i=1}^{2N} |t-v_i|^{1/2}}\,\mathrm{d}t, \tag{3.4}$$

for $j = 0, 1, \ldots, N$ and $k = 1, 2, \ldots, N$. We then note that because of the centreline symmetry the mapping function $\Sigma(\zeta)$ must satisfy the condition $\Sigma(v_{2k-1}) = \Sigma(v_k)$, which in view of (3.3) and (3.4) yields

$$\sum_{j=0}^{N} a_j I_{jk} = 0, \quad k = 1, 2, \ldots, N. \tag{3.5}$$

Furthermore, the real part of $\Sigma(\zeta)$ must jump by -1 as ζ crosses the pole $\zeta = 1$ from left to right (see figure 2), which implies in turn that

$$\sum_{j=0}^{N} a_j = \prod_{k=1}^{2N} (1-v_k)^{1/2}. \tag{3.6}$$

Relations (3.5) and (3.6) thus give a system of $N+1$ linear equations that can be easily solved for the $N+1$ coefficients a_j, once the set of $2N$ parameters $\{v_i\}$ is given.

Now that the two mapping functions $\Phi(\zeta)$ and $\Sigma(\zeta)$ have been determined, it becomes a trivial matter to find the bubble shapes. From (2.22), (2.23), (3.1) and (3.3), it follows that the interface $\mathscr{C}_k$, for $k = 1, \ldots, N$, is given by the following parametric equations:

$$x_k(s) = x_0^k + \frac{1}{\pi}\tanh^{-1} s, \tag{3.7}$$

$$y_k(s) = \frac{(-1)^{N+k+1}}{\pi} \int_{v_{2k-1}}^{s} \frac{\sum_{j=0}^{N} a_j t^j}{(1-t^2)\prod_{j=1}^{2N} |t-v_j|^{1/2}}\,\mathrm{d}t, \tag{3.8}$$

where $s \in \mathscr{I}_k$ and

$$x_0^k = \frac{(-1)^N}{\pi} \sum_{l=1}^{k-1} (-1)^l \int_{v_{2l}}^{v_{2l+1}} \frac{\sum_{j=0}^{N} a_j t^j}{(1-t^2)\prod_{j=1}^{2N} |t-v_j|^{1/2}}\,\mathrm{d}t. \tag{3.9}$$

In (3.7) an overall additive constant has been omitted for brevity. (We remark parenthetically that the several factors of -1 in (3.8) and (3.9) arise from the crossing of two square-root branch points as ζ moves from one interval $\mathscr{I}_k$ to the next.) Expressions (3.7)–(3.9) thus give a general solution for the problem of N steadily moving bubbles with centreline symmetry. In the formulation above, in order to specify a solution completely one must provide $2N$ values for the parameters v_j. The solutions could alternatively be specified if we prescribed the bubble areas and their separation, from which the values of the v_j could in principle be determined (with the value of one given v_j being chosen arbitrarily). For convenience, we prefer however to work directly with the v_j.

In the special cases of $N = 1$ and $N = 2$, the solutions above can can be written in closed form and will be discussed separately in the next two subsections. For $N > 2$, on the other hand, one must resort to numerical integration in order to compute the interface shapes. An example solution for $N = 3$ with $v_1 = -0.95$, $v_2 = 0.65$, $v_3 = -0.6$, $v_4 = -0.2$, $v_5 = 0.2$ and $v_6 = 0.4$ is shown in figure 4. Note, in particular, that if the parameters v_j are chosen in such way that the intervals $\mathscr{I}_k$ are symmetrically located about the point $\zeta = 0$, then the overall solution will be symmetrical about the y-axis

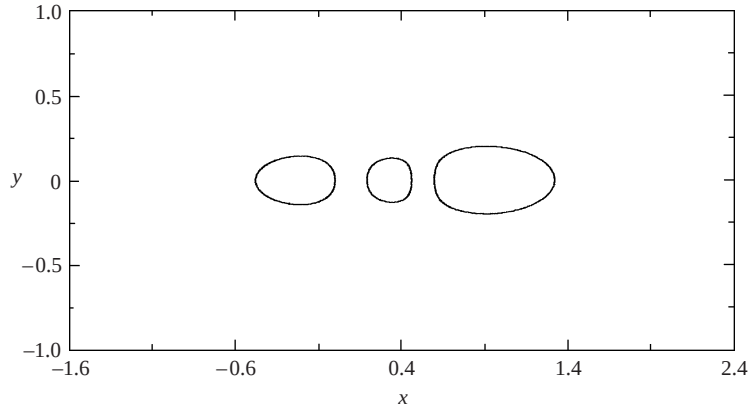

FIGURE 4. Solution for three unequal bubbles with centerline symmetry. Here the parameters are $v_1 = -0.95$, $v_2 = 0.65$, $v_3 = -0.6$, $v_4 = -0.2$, $v_5 = 0.2$ and $v_6 = 0.4$.

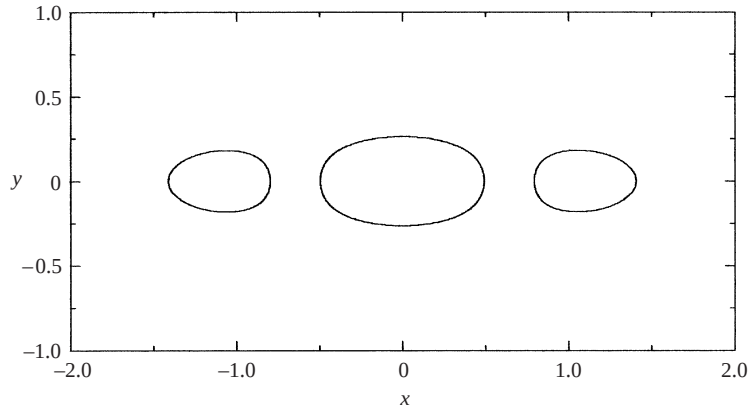

FIGURE 5. Solution for three bubbles with both the centreline and downstream–upstream symmetries. Here $v_6 = -v_1 = 0.9$, $v_5 = -v_2 = 0.7$ and $v_4 = -v_3 = 0.2$.

and the flow will accordingly have a downstream–upstream symmetry. In figure 5 we show a solution for this case with $N = 3$.

3.2. *The Taylor–Saffman bubble*

In the case that $N = 1$ our general solution discussed above should reproduce the solution originally obtained by Taylor & Saffman (1959) for a single symmetrical bubble in a Hele-Shaw channel. For completeness, and as a test of our formulation, we will show below that the Taylor–Saffman bubble can indeed be obtained as a special case of the general solution given in (3.7) and (3.8).

First we note that setting $N = k = 1$ in (3.9) gives $x_0 = 0$ so that (3.7) yields simply

$$x(s) = \frac{1}{\pi} \tanh^{-1} s. \tag{3.10}$$

Next we note that because a single centreline symmetric bubble must also have fore-and-aft symmetry we can, without loss of generality, set $v_2 = -v_1 = v$, where $0 < v < 1$, so that from (3.5) and (3.6) we have $a_0 = 0$ and $a_1 = \sqrt{1 - v^2}$. Using these

facts in (3.8) with $N = k = 1$, one then finds

$$y(s) = -\frac{\sqrt{1-v^2}}{\pi}\int_{-v}^{s}\frac{t\,\mathrm{d}t}{(1-t^2)\sqrt{v^2-t^2}}, \tag{3.11}$$

which upon integration becomes

$$y(s) = \frac{1}{\pi}\tan^{-1}\sqrt{\frac{v^2-s^2}{1-v^2}}. \tag{3.12}$$

Eliminating the parameter s from (3.10) and (3.12) then finally gives

$$x = \frac{1}{\pi}\tanh^{-1}\{\sin^2(\pi\lambda) - \cos^2(\pi\lambda)\tan^2(\pi y)\}^{1/2}, \tag{3.13}$$

where λ is the bubble maximum half-width, being related to our original parameter by $v = \sin\pi\lambda$. Equation (3.13) is precisely the formula obtained by Taylor & Saffman (1959). We note in passing that this equation can be more compactly rewritten as

$$x = \frac{1}{\pi}\cosh^{-1}\left[\frac{\cos\pi y}{\cos\pi\lambda}\right]. \tag{3.14}$$

Next we discuss the case of two bubbles for which there also exists an analytic solution.

3.3. *Pair of bubbles*

We now consider the problem of two unequal centreline-symmetric bubbles moving steadily in a Hele-Shaw cell. In this case, as we will see below, the bubble shapes can also be written in closed form in terms of elliptic integrals. A preliminary description of these solutions has been given in an earlier paper by the author (Vasconcelos 2000). Our aim here is to present a complete derivation of such solutions.

Setting $N = 2$ and $k = 1$ in (3.7)–(3.9) we find that the first bubble is given by

$$x_1(s) = \frac{1}{\pi}\tanh^{-1}s, \tag{3.15}$$

$$y_1(s) = \frac{1}{\pi}\int_{v_1}^{s}\frac{a+bt+ct^2}{(1-t^2)\sqrt{t(v_1-t)(v_3-t)(v_4-t)}}\,\mathrm{d}t, \tag{3.16}$$

where $v_1 \leqslant s \leqslant 0$. Similarly, for the second bubble ($N = k = 2$) we have

$$x_2(s) = x_0 + \frac{1}{\pi}\tanh^{-1}s, \tag{3.17}$$

$$y_2(s) = -\frac{1}{\pi}\int_{v_3}^{s}\frac{a+bt+ct^2}{(1-t^2)\sqrt{t(t-v_1)(t-v_3)(v_4-t)}}\,\mathrm{d}t, \tag{3.18}$$

where $v_3 \leqslant s \leqslant v_4$ and the constant x_0 is given by

$$x_0 = -\frac{1}{\pi}\int_{0}^{v_3}\frac{a+bt+ct^2}{(1-t^2)\sqrt{t(t-v_1)(v_3-t)(v_4-t)}}\,\mathrm{d}t, \tag{3.19}$$

as one readily sees after setting $N = k = 2$ in (3.9). The coefficients a, b and c above are determined from the following requirements:

$$y_1(0) = y_2(v_4) = 0, \tag{3.20}$$

$$a + b + c = \sqrt{(1-v_1)(1-v_3)(1-v_4)}. \tag{3.21}$$

The two conditions in (3.20) enforce the bubble centreline symmetry, while (3.21) corresponds to (3.6). In obtaining the formulas above we have also made use of the third degree of freedom of Riemann's theorem and have set $v_2 = 0$.

The integrals in (3.16), (3.18) and (3.19) can all be expressed in terms of elliptic integrals (Byrd & Friedman 1971). This requires, however, a lengthy calculation that we defer to Appendix A. Here we shall simply quote the results, but before doing that we need to introduce some notation. First we define the function

$$H(\varphi, u, v, k) = G(\varphi, u, k) - G(\varphi, v, k), \tag{3.22}$$

where

$$G(\varphi, n, k) = \sqrt{(1-n)(n-k^2)/n}\left[\Pi(\varphi, n, k) - \frac{\Pi(n,k)}{K} F(\varphi, k)\right]. \tag{3.23}$$

Here $F(\varphi, k)$ and $\Pi(\varphi, n, k)$ are the normal elliptic integrals of first and third kinds, respectively, with $K \equiv K(k) \equiv F(\pi/2, k)$ and $\Pi(n,k) \equiv \Pi(\pi/2, n, k)$ being the complete elliptic integrals of first and third kinds, respectively. In the above we have adopted Legendre's notation for the elliptic integrals in which φ is the *argument*, k is called the *modulus*, and n is referred to as the *parameter* (Byrd & Friedman 1971). Next we note that the function H defined above satisfies the identity

$$H(\varphi, u, v, k) = H(\psi, r, t, k), \tag{3.24}$$

where

$$\cot\psi = k' \tan\varphi, \quad r = \frac{k^2 - v}{1 - v}, \quad t = \frac{k^2 - u}{1 - u}, \tag{3.25}$$

with $k' = \sqrt{1-k^2}$ being the so-called *complementary modulus*. (For a proof, see Appendix B.)

Now using the result given in (A 27) for the integral appearing in (3.16), we then find

$$y_1(s) = \frac{1}{\pi} H(\varphi_1(s), m, n, k), \tag{3.26}$$

where

$$\varphi_1(s) = \sin^{-1}\sqrt{\frac{n - m + (m+n-2)s}{n - m - (n+m-2mn)s}}. \tag{3.27}$$

Similarly, using (A 28) in (3.18) we obtain for the y-coordinate of the second bubble

$$y_2(s) = \frac{1}{\pi} H(\varphi_2(s), p, q, k), \tag{3.28}$$

where

$$\varphi_2(s) = \sin^{-1}\sqrt{\frac{p - q + (p+q)s}{2pqs}}. \tag{3.29}$$

Finally, inserting (A 37) into (3.19) one sees that the constant x_0 reads simply

$$x_0 = \frac{1}{2K}[F(\beta_q, k') - F(\beta_p, k')], \tag{3.30}$$

with β_q being given by

$$\beta_q = \sin^{-1}\sqrt{\frac{q - k^2}{qk'^2}}, \tag{3.31}$$

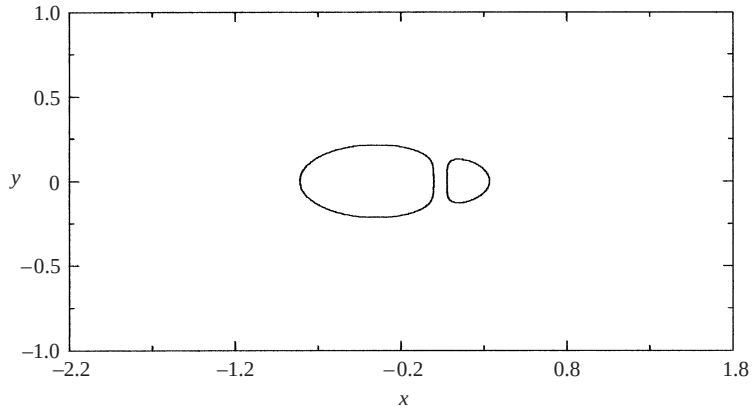

FIGURE 6. A pair of centreline-symmetric bubbles with $k = 0.46$, $p = 0.22$ and $q = 0.5$.

and similar expression for β_p. The five parameters k^2, m, n, p and q introduced above are of course not all independent. As shown in Appendix A, m and n are related to p and q, respectively, via the equations

$$m = \frac{k^2(p-1)}{p-k^2}, \quad n = \frac{k^2(q-1)}{q-k^2}. \tag{3.32}$$

The original parameters v_1, v_3 and v_4 can also be expressed in terms of k, p and q; see (A 15).

We have thus obtained a three-parameter family of solutions for a pair of centreline-symmetric bubbles. In describing these solutions we can use either (k, m, n) or (k, p, q) as our set of free parameters, with these parameters taking values in the ranges

$$m < n < 0 < k^2 < 1 \quad \text{and} \quad 0 < k^2 < p < q < 1. \tag{3.33}$$

Passing from one representation to another is accomplished by the identity (3.24). For example, setting $u = m$, $v = n$, $r = k^2/q$ and $t = k^2/p$ in (3.24) we can express (3.26) in terms of $H(\psi_1, k^2/q, k^2/p, k)$, where $\cot\psi_1 = k' \tan\varphi_1$. Similarly we can rewrite (3.28) in terms of $H(\psi_2, k^2/n, k^2/m, k)$, with $\cot\psi_2 = k' \tan\varphi_2$. In figure 6 we show a solution with $k = 0.46$, $p = 0.22$ and $q = 0.5$.

It is perhaps worth pointing out that in either limit that one of the bubbles shrinks to zero or that the separation between the two bubbles vanishes (so that they merge into a single bubble) our two-bubble solution correctly reproduces the Taylor–Saffman bubble. For example, the latter limit corresponds to taking $k \to 1$ and $mn = 1$. Using the special values for $F(\varphi, 1)$ and $\Pi(\varphi, m, 1)$ one can show that in this limit (3.26) does indeed give (3.12). We will however spare the reader the mathematical details.

As already mentioned, analytic solutions for a pair of bubbles were presented (without derivation) by the author in an earlier publication (Vasconcelos 2000). For the benefit of the reader who may wish to compare these solutions with the one given above, we note here that the parameters p and q used in the present paper correspond to k^2/q and k^2/p, respectively, in the notation of Vasconcelos (2000).

3.4. *Finger with bubbles*

Notice that if the first bubble in figure 1(a) becomes infinitely elongated, while the other bubbles remain finite, the resulting configuration corresponds to an advancing finger with several bubbles moving ahead of the finger tip. Exact solutions for a finger

with multiple bubbles have been obtained previously by the author (Vasconcelos 1999). Here we wish to point out that these finger-bubble solutions can be viewed as a particular case of the generic N-bubble solution presented above. In fact, solutions for a finger with $N-1$ bubbles can be obtained by taking the limit $\gamma_1 = v_1 = -1$ and $v_2 = 0$ in the formulas of § 3.1 and performing some additional algebra, the details of which will not be given here. For a finger with a single bubble, in particular, an analytic solution in terms of elliptic integrals can be obtained (Vasconcelos 2000) as a special case of the two-bubble solution described in the preceding subsection.

4. Bubbles with fore-and-aft symmetry

We will now consider the case shown in figure 3 where the bubbles have fore-and-aft symmetry. First we will present a general solution in integral form for an arbitrary number N of bubbles and then proceed to discuss the case $N = 1$ for which there also exists an analytic solution in terms of elliptic integrals.

4.1. *Generic solutions*

We begin by considering the conformal mapping $\tilde{W} = \Sigma(\zeta)$. Here the flow domain in the $\tilde{W}$-plane is the half-strip $-1 < \tilde{\phi} < 1$, $\tilde{\psi} > 0$ shown in figure 3(*c*). The conformal mapping from the upper half-ζ-plane onto this half-strip is effected by the function

$$\Sigma(\zeta) = -\frac{2}{\pi}\cos^{-1}\zeta. \tag{4.1}$$

Next we turn to the mapping $W = \Phi(\zeta)$. The domain in the W-plane corresponds to the half-strip $\phi < 0$, $-1 < \psi < 1$ with N horizontal slits, as shown in figure 3(*b*). This domain can also be viewed as a degenerate polygon and so the corresponding conformal mapping $W = \Phi(\zeta)$ can be found from the Schwarz–Christoffel formula:

$$\Phi(\zeta) = \Phi_0 + \frac{\mathrm{i}C}{\pi}\int_{\zeta_0}^{\zeta} \frac{\prod_{j=1}^{N}(\zeta-\gamma_j)}{\sqrt{1-\zeta^2}\prod_{j=1}^{2N}(\zeta-v_j)^{1/2}}\,\mathrm{d}\zeta. \tag{4.2}$$

Here we have used the three degrees of freedom of Riemmann's mapping theorem to map $\zeta = \pm 1$ onto $z = \mp\mathrm{i}$ and $\zeta = \infty$ onto $z = \infty$. As in § 3.1, it is convenient to expand the numerator in (4.2) and so we write

$$\Phi(\zeta) = -\mathrm{i} + \frac{2\mathrm{i}}{\pi}\int_{-1}^{\zeta} \frac{\sum_{j=0}^{N} a_j\zeta^j}{\sqrt{1-\zeta^2}\prod_{i=1}^{2N}(\zeta-v_i)^{1/2}}\,\mathrm{d}\zeta, \tag{4.3}$$

where we have chosen $\zeta_0 = -1$ so that $\Phi_0 = -\mathrm{i}$.

The coefficients a_j above are determined as follows. First we must have $a_N = 1$, so that $\Phi(\zeta)$ will display the appropriate behaviour at infinity: $\Phi(\zeta) \approx (2\mathrm{i}/\pi)\ln\zeta$ as $\zeta \to \infty$. (To see that $\Phi(\zeta)$ must indeed have such behaviour, let $\zeta = R\mathrm{e}^{\mathrm{i}\theta}$, with $R \gg 1$ and then notice that as θ varies from $\theta = 0$ to $\theta = \pi$ the imaginary part of $\Phi(\zeta)$ must vary by -2.) The other coefficients a_j, for $j = 0, 1, \ldots, N-1$, are determined from the parameters v_j via a procedure similar to that used in § 3.1. Let us then introduce the quantities J_{jk}

$$J_{jk} = \int_{v_{2k-1}}^{v_{2k}} \frac{t^j\,\mathrm{d}t}{\sqrt{1-t^2}\prod_{i=1}^{2N}|t-v_i|^{1/2}}, \tag{4.4}$$

for $j = 0, 1, \ldots, N$ and $k = 1, \ldots, N$. Now, from the requirement of fore-and-aft sym-

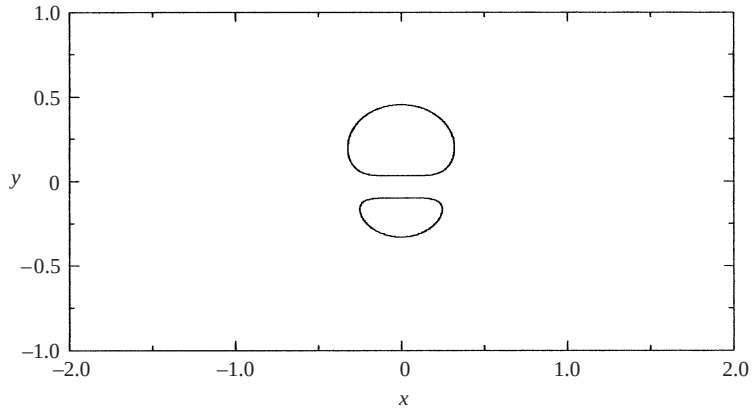

FIGURE 7. A pair of bubbles with fore-and-aft symmetry. The parameters are $v_1 = -0.9$, $v_2 = 0.2$, $v_3 = 0.205$ and $v_4 = 0.8$.

metry it follows that $\Phi(v_{2k-1}) = \Phi(v_k)$, which in view of (4.3) and (4.4) implies

$$\sum_{j=0}^{N} a_j J_{jk} = 0, \quad k = 1, 2, \ldots, N. \tag{4.5}$$

Equation (4.5) thus gives a system of N linear equations for the N unknown coefficients a_j, for $j = 0, \ldots, N-1$.

The bubble shapes are now readily obtained from (2.22), (2.23), (4.1) and (4.3). We then find that the interface $\mathscr{C}_k$ for the kth bubble is given by the equations

$$x_k(s) = \frac{(-1)^{N+k+1}}{\pi} \int_{v_{2k-1}}^{s} \frac{\sum_{j=0}^{N} a_j t^n}{\sqrt{1-t^2} \prod_{j=1}^{2N} |t - v_j|^{1/2}} \, \mathrm{d}t, \tag{4.6}$$

$$y_k(s) = y_0^k + \frac{1}{\pi} \cos^{-1} s, \tag{4.7}$$

where $s \in \mathscr{I}_k$, with $\mathscr{I}_k$ as defined in (2.20) and

$$y_0^k = \frac{(-1)^{N+1}}{\pi} \sum_{l=0}^{k-1} (-1)^l \int_{v_{2l}}^{v_{2l+1}} \frac{\sum_{j=0}^{N} a_j t^n}{\sqrt{1-t^2} \prod_{j=1}^{2N} |t - v_j|^{1/2}} \, \mathrm{d}t. \tag{4.8}$$

In (4.8) we have, for conciseness, introduced the notation $v_0 = -1$.

Equations (4.6)–(4.8) thus give a $2N$-parameter family of solutions for N bubbles with fore-and-aft symmetry moving 'side-by-side' in a Hele-Shaw channel. From a physical standpoint, the $2N$ free-parameters correspond, of course, to the bubble sizes and the vertical separations between adjacent bubbles. An example of a solution for $N = 2$ is shown in figure 7. Note, in particular, that if the intervals $\mathscr{I}_k$ are symmetrically placed about $\zeta = 0$, then the overall solution will be symmetrical about the channel centreline. In this case, when there is an odd number of bubbles the bubble at the centre will itself be centreline-symmetric, while each off-centre bubble will have a corresponding mirror image. A solution for such a case with $N = 3$ is given in figure 8. On the other hand, if there is an even number N of bubbles with fore-and-aft symmetry in a centreline-symmetric flow, then the problem can be reduced to that of $N/2$ bubbles in a channel with one half of the original width.

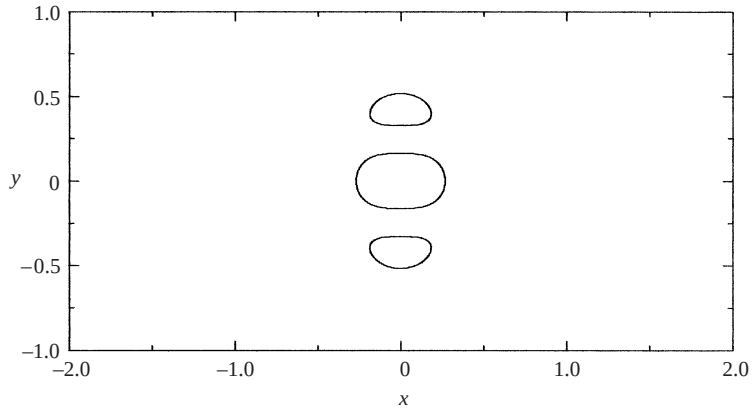

FIGURE 8. Three bubbles with fore-and-aft symmetry in a flow symmetric about the channel centreline. Here $v_4 = -v_1 = 0.95$ and $v_3 = -v_2 = 0.001$.

4.2. *Single asymmetrical bubble*

For $N = 1$ the solution of the preceding subsection describes a single bubble that has fore-and-aft symmetry but that in general is not symmetrical about the channel centreline. Exact solutions for such bubbles were first obtained by Tanveer (1987) using conformal mappings between doubly connected domains. Our formalism has however the advantage of being somewhat simpler for it involves only conformal mappings between simply connected regions. Moreover, our method yields a closed-form solution for the bubble in terms of elliptic integrals, as shown below.

Let us first compute the bubble x-coordinate. Setting $N = k = 1$ in equation (4.6) yields

$$x(s) = \frac{1}{\pi}\int_{v_1}^{s} \frac{b - t}{\sqrt{(1 - t^2)(t - v_1)(v_2 - t)}}\,\mathrm{d}t, \tag{4.9}$$

where $b = -a_0$ and $-1 < v_1 \leqslant s \leqslant v_2 < 1$. As in § 3.3, the integral above can be written in terms of elliptic integrals (Byrd & Friedman 1971). The final result is

$$x(s) = \frac{1}{\pi}\,G(\varphi(s), n, k), \tag{4.10}$$

where the function $G(\varphi, n, k)$ is as defined in (3.23), the argument φ is given by

$$\varphi(s) = \sin^{-1}\sqrt{\frac{2n - k^2(1 - s)}{nk^2(1 - s)}}, \tag{4.11}$$

and the modulus k and the parameter n satisfy

$$0 < n < k^2 < 1. \tag{4.12}$$

In terms of k and n the original parameters v_1 and v_2 read

$$v_1 = 1 - \frac{2n}{k^2}, \quad v_2 = 1 - \frac{2nk'^2}{k^2(1 - n)}. \tag{4.13}$$

Now we turn to the bubble y-coordinate. After taking $N = k = 1$ in (4.7) and (4.8) one finds

$$y(s) = y_0 + \frac{1}{\pi}\cos^{-1} s, \tag{4.14}$$

where

$$y_0 = -\frac{1}{\pi}\int_{-1}^{v_1} \frac{b-t}{\sqrt{(1-t^2)(t-v_1)(t-v_2)}}\,\mathrm{d}t. \tag{4.15}$$

This integral can also be expressed in terms of elliptic integrals and after some tedious algebra one obtains

$$y_0 = -\frac{F(\beta,k)}{K(k)}, \tag{4.16}$$

where

$$\beta = \sin^{-1}\sqrt{\frac{k^2-n}{k^2(1-n)}}. \tag{4.17}$$

Equations (4.10), (4.11), (4.14) and (4.16) thus give a two-parameter family of exact solutions for a single bubble with fore-and-aft symmetry but non-symmetric (in general) about the channel centreline. Note, in particular, that in the event that the bubble becomes symmetrical about the centreline the solution above should reproduce the Taylor–Saffman bubble given in (3.13). Using the fact that the symmetric case corresponds to $n = 1 - k'$ and resorting to certain relations between the elliptic integrals, one can show that the solution above does indeed reproduce (3.13). We remark, however, that it is easier to rederive (3.13) by first setting $b = 0$ and $v_2 = -v_1 = v$ in (4.9), performing the integration, and then combining the result with (4.14).

4.3. *Multiple fingers*

If in figure 1(*b*) we consider the limit in which the vertical axis of symmetry recedes to $-\infty$, then all the bubbles become infinitely elongated and we arrive at a situation where several fingers penetrate simultaneously into a Hele-Shaw channel. Exact solutions for multiple fingers in a Hele-Shaw cell at zero surface tension have recently been reported by Vasconcelos (1998, 2001). Here we note that these multifinger solutions can be obtained as a particular case of the generic bubble solution given in § 4.1 in the limit that $v_1 \to -1$, $v_{2N} \to 1$ and $v_{2j} \to v_{2j+1}$ for $j = 1,\ldots,N-1$. In such case, the square-root branch points in (4.2) merge pairwise into single poles so that $\Phi(\zeta)$ will be given as a sum of logarithmic terms. Carrying out the subsequent calculation, one then obtains a multifinger solution where the x-coordinate along each of the fingers can be written explicitly as a sum of logarithmic terms in the corresponding y-coordinate, as found previously by Vasconcelos (1998).

5. Conclusions

We have presented exact solutions for the problem of N bubbles moving with a constant velocity in a Hele-Shaw channel when surface tension is neglected. Depending upon the symmetry displayed by the bubbles these solutions can be classified into two groups: (i) solutions where the bubbles are symmetric about the channel centreline and (ii) solutions in which the bubbles have fore-and-aft symmetry. Our solutions have been constructed via conformal mapping techniques and are in general written in integral form. We have however found solutions in closed form in terms of elliptic integrals for the following two important cases: (i) a pair of centreline-symmetric bubbles and (ii) a single bubble with fore-and-aft symmetry but non-symmetric about the centreline.

Although the solutions presented here are for the idealized case of zero surface

tension, they are nevertheless of physical significance. For instance, it has been found (Vasconcelos 2000) that our two-bubble solution with zero surface tension describes remarkably well shapes observed in the experiments conducted by Ikeda & Maxworthy (1990) on the problem of a large bubble with a small one attached to its nose. The existence of this analytic solution for a pair of bubbles thus opens up the prospects for further studies concerning the selection problem in this case. Moreover, the wealth of bubble solutions described in the present paper may explain, in part, the plethora of shapes observed by Maxworthy (1986) in his experiment on rising bubbles in a Hele-Shaw cell. Some of those shapes do indeed bear some resemblance to solutions presented here.

The solutions reported in the present paper are rather general in the sense that all previously known steady solutions in an unbounded channel geometry are particular cases of our solutions. An attempt is now being made to find even more general solutions by removing the symmetry requirement imposed on the bubbles. The problem in this case becomes much harder for now the fluid domain can no longer be reduced to a simply connected region. Our method of solution still applies here, in a formal sense, but the construction of the actual conformal mappings $\Phi(\zeta)$ and $\Sigma(\zeta)$ seems to be a difficult task. Another possible generalization is to consider the case of periodic solutions with several bubbles per period cell. A class of such solutions for multiple centreline-symmetric bubbles has already been obtained (Vasconcelos 1994) that generalizes the solution found by Burgess & Tanveer (1991) for a periodic array of identical bubbles. We are now working out an extension of these periodic solutions that should, in the limit that the cell period becomes infinitely large, reproduce our N-bubble solution given in § 3.1. We are also investigating periodic solutions having multiple bubbles with fore-and-aft symmetry per unit cell.

As a concluding remark, we note that up to this date the only known time-dependent solutions in the rectangular Hele-Shaw cell are for the case in which the viscous fluid occupies a simply connected region. (These solutions describe a single interface that asymptotically evolves to one or more fingers.) We are thus currently investigating the existence of time-evolving solutions for bubbles. If such solutions do exist, one would thus expect to find a class of time-dependent solutions that will asymptotically approach the steady bubble solutions reported in the present paper. We hope to be able to report some progress on this difficult problem in the near future.

I would like to acknowledge Leo P. Kadanoff for introducing me, several years ago, to the beautiful subject of Hele-Shaw flows. This work was supported in part by FINEP, CNPq, and PRONEX under grant number 76.97.1004.00.

Appendix A. Elliptic integrals

We first consider the integral

$$I_1(s) = \int_{v_1}^{s} \frac{a + bt + ct^2}{(1 - t^2)\sqrt{-t(t - v_1)(v_3 - t)(v_4 - t)}}\, \mathrm{d}t, \tag{A 1}$$

where $-1 < v_1 < s \leqslant 0 < v_3 < v_4 < 1$ and the coefficients a, b and c satisfy the condition

$$a + b + c = \sqrt{(1 - v_1)(1 - v_3)(1 - v_4)}. \tag{A 2}$$

The integral above can be expressed in terms of elliptic integrals (Byrd & Friedman 1971). After some simplification one then finds

$$I_1(s) = A_{nk}[B_1 F(\varphi_1(s),k) + B_2 \Pi(\varphi_1(s),m,k) - \Pi(\varphi_1(s),n,k)], \tag{A 3}$$

where

$$\varphi_1(s) = \sin^{-1}\sqrt{\frac{v_4(s-v_1)}{v_1(s-v_4)}}, \tag{A 4}$$

$$k^2 = \frac{v_1(v_3-v_4)}{v_4(v_3-v_1)}, \quad m = \frac{v_1(1+v_4)}{v_4(1+v_1)}, \quad n = \frac{v_1(1-v_4)}{v_4(1-v_1)}, \tag{A 5}$$

$$B_1 = \frac{1-v_1}{v_4-v_1}\left[1+\frac{1-v_4}{1+v_4}X-(1-v_4)Y\right], \quad B_2 = \frac{(1-v_1)(1-v_4)}{(1+v_1)(1+v_4)}X, \tag{A 6}$$

with the coefficient A_{nk} in (A 3) being defined as

$$A_{nk} = \sqrt{(1-n)(n-k^2)/n}. \tag{A 7}$$

Here we have for convenience introduced the notation $X = (a-b+c)/(a+b+c)$ and $Y = 2a/(a+b+c)$.

The second integral of interest is

$$I_2(s) = \int_{v_3}^{s} \frac{a+bt+ct^2}{(1-t^2)\sqrt{t(t-v_1)(t-v_3)(v_4-t)}}\,\mathrm{d}t, \tag{A 8}$$

where now $v_3 < s \leqslant v_4$. In this case, we find

$$I_2(s) = A_{qk}[C_1 F(\varphi_2(s),k) - C_2 \Pi(\varphi_2(s),p,k) + \Pi(\varphi_2(s),q,k)], \tag{A 9}$$

where A_{qk} is as defined in (A 7) and

$$\varphi_2(s) = \sin^{-1}\sqrt{\frac{v_4(s-v_3)}{s(v_4-v_3)}}, \tag{A 10}$$

$$p = \frac{v_4-v_3}{v_4(1+v_3)}, \quad q = \frac{v_4-v_3}{v_4(1-v_3)}, \tag{A 11}$$

$$C_1 = \frac{v_3-1}{v_3}[1+X-Y], \quad C_2 = \frac{1-v_3}{1+v_3}X. \tag{A 12}$$

Among the five parameters k, m, n, p and q introduced above, of course only three of them are independent (corresponding to the three original parameters v_i). Indeed, from the definitions above one easily finds that the parameters m and n are related to p and q, respectively, via the equations

$$m = \frac{k^2(p-1)}{p-k^2}, \quad n = \frac{k^2(q-1)}{q-k^2}. \tag{A 13}$$

We can thus use either k, m and n or k, p and q as our set of independent parameters, with these parameters ranging over the intervals

$$m < n < 0 < k^2 < 1 \quad \text{and} \quad 0 < k^2 < p < q < 1, \tag{A 14}$$

as can be easily verified from the definitions above. The original parameters v_i can

also be expressed in terms of the new parameters and here one finds

$$v_1 = \frac{k^2(q-p)}{k^2(q+p)-2pq}, \quad v_3 = \frac{q-p}{q+p}, \quad v_4 = \frac{q-p}{p+q-2pq}, \tag{A 15}$$

which in view of (A 13) can alternatively be written in terms of k, m, and n. Using (A 15) in (A 4) and (A 10), we can rewrite the arguments φ_1 and φ_2 in terms of the new parameters:

$$\varphi_1(s) = \sin^{-1}\sqrt{\frac{n-m+(m+n-2)s}{n-m-(n+m-2mn)s}}, \tag{A 16}$$

$$\varphi_2(s) = \sin^{-1}\sqrt{\frac{p-q+(p+q)s}{2pqs}}. \tag{A 17}$$

We now require that $I_1(0) = I_2(v_4) = 0$, so as to ensure centreline symmetry; see (3.20). In view of (A 3) and (A 9) these requirements imply that

$$B_1K + B_2\Pi(m,k) - \Pi(n,k) = 0, \tag{A 18}$$

$$C_1K - C_2\Pi(p,k) + \Pi(q,k) = 0. \tag{A 19}$$

This gives a system of two linear equations that can be easily solved for the two unknowns X and Y. Despite this apparent simplicity, the expressions obtained for X and Y after a direct solution of the system above are very cumbersome and a great deal of manipulation is required to bring them into a more manageable form. For example, after tedious algebra one finds that X can be conveniently written as

$$X = \frac{q(1-p)}{p(1-q)}\left[\frac{(1-n)\Pi(n,k)+(1-q)\Pi(q,k)-K}{(1-m)\Pi(m,k)+(1-p)\Pi(p,k)-K}\right]. \tag{A 20}$$

This expression can be further simplified if we note the identity

$$(1-n)\Pi(n,k)+(1-q)\Pi(q,k) = K + \frac{\pi}{2}\frac{1-q}{A_{qk}}, \tag{A 21}$$

which is valid whenever n and q are related as in (A 13). (A similar expression holds, of course, if we replace n and q with m and p, respectively.) Using (A 21) in (A 20) we then finally obtain

$$X = \frac{qA_{pk}}{pA_{qk}}. \tag{A 22}$$

Similarly one finds that the solution for Y can be written as

$$Y = 1 + \frac{qA_{pk}}{A_{qk}} + \frac{q-p}{2pA_{qk}K}[A_{qk}\Pi(q,k) - A_{pk}\Pi(p,k)]. \tag{A 23}$$

Next we note that in view of (A 18) and (A 19) equations (A 3) and (A 9) can be rewritten as

$$I_1 = \frac{A_{nk}}{A_{mk}}B_2G(\varphi_1,m,k) - G(\varphi_1,n,k), \tag{A 24}$$

$$I_2 = G(\varphi_2,q,k) - \frac{A_{qk}}{A_{pk}}C_2G(\varphi_2,p,k), \tag{A 25}$$

where the function $G(\varphi,n,k)$ is as defined in (3.23). (Here the dependence on s has

been omitted for brevity.) Now using (A 22) together with (A 6) and (A 12) we find that the coefficients B_2 and C_2 are given by

$$B_2 = \frac{A_{mk}}{A_{nk}}, \quad C_2 = \frac{A_{pk}}{A_{qk}}, \tag{A 26}$$

so that after inserting these expressions into (A 24) and (A 25) we finally obtain

$$I_1 = H(\varphi_1, m, n, k), \tag{A 27}$$

$$I_2 = H(\varphi_2, q, p, k), \tag{A 28}$$

where the function $H(\varphi, u, v, k)$ has been defined in (3.22).

The last integral we need to consider is

$$I_3 = \int_0^{v_3} \frac{a + bt + ct^2}{(1-t^2)\sqrt{t(t-v_1)(v_3-t)(v_4-t)}}\,\mathrm{d}t, \tag{A 29}$$

which appears in the definition of the constant x_0 given in (3.19). In terms of elliptic integrals the above integral reads

$$I_3 = D[e_1 K' + e_2 \Pi(u, k') - e_3 \Pi(v, k')], \tag{A 30}$$

where

$$D = \frac{a+b+c}{\sqrt{v_4(v_3-v_1)}}, \quad u = \frac{v_3(1-v_1)}{v_3-v_1}, \quad v = \frac{v_3(1+v_1)}{v_3-v_1} \tag{A 31}$$

$$e_1 = \frac{1}{1-v_1} + \frac{X}{1+v_1} - Y, \quad e_2 = \frac{v_1}{1-v_1}, \quad e_3 = \frac{v_1 X}{1+v_1}. \tag{A 32}$$

In (A 30) we have used the standard notation $K' \equiv K(k')$. Using the expressions for X and Y given in (A 22) and (A 23), one finds after some simplification that I_3 can be written as

$$I_3 = \frac{A_{pk}}{(p-k^2)K}\,[k^2 K K' - k^2 K \Pi(v, k') - (k^2 - p) K' \Pi(p, k)]$$

$$- \frac{A_{qk}}{(q-k^2)K}\,[k^2 K K' - k^2 K \Pi(u, k') - (k^2 - q) K' \Pi(q, k)]. \tag{A 33}$$

This expression can be simplified further if we note that u is related to q and k^2 via

$$u = \frac{q - k^2}{q}, \tag{A 34}$$

in which case we have the identity (Byrd & Friedman 1971)

$$k^2 K K' - k^2 K \Pi(u, k') - (k^2 - q) K' \Pi(q, k) = \frac{\pi}{2} \frac{q - k^2}{A_{qk}} F(\beta_q, k'), \tag{A 35}$$

where

$$\beta_q = \sin^{-1} \sqrt{\frac{q - k^2}{q k'^2}}. \tag{A 36}$$

(Similar expressions hold if we replace u and q with v and p, respectively.) Using (A 35) and the similar identity in terms of v and p, one then immediately sees that (A 33) becomes simply

$$I_3 = \frac{\pi}{2K}[F(\beta_p, k') - F(\beta_q, k')]. \tag{A 37}$$

Appendix B

Here we shall prove formula (3.24) for the function $H(\varphi, m, n, k)$. To do this, we will need several identities involving elliptic integrals (Byrd & Friedman 1971):

$$\Pi(q,k) + \Pi(k^2/q,k) = K + \frac{\pi}{2}\frac{1}{A_{qk}}, \tag{B 1}$$

$$\Pi(\varphi,q,k) + \Pi(\varphi,k^2/q,k) = F(\varphi,k) + \frac{1}{A_{qk}}\tan^{-1}\left[\frac{A_{qk}\tan\varphi}{\sqrt{1-k^2\sin^2\varphi}}\right], \tag{B 2}$$

$$\Pi(\varphi,q,k) + \Pi(\psi,q,k) = \Pi(q,k) - \frac{1}{A_{qk}}\tan^{-1}\left[\frac{q-k^2}{A_{qk}}\sin\varphi\sin\psi\right], \tag{B 3}$$

$$(1-n)\Pi(\varphi,n,k) + (1-q)\Pi(\varphi,q,k) = F(\varphi,k) + \frac{1-q}{A_{qk}}\left\{\tan^{-1}\left[\frac{k'^2\tan\varphi}{A_{qk}\sqrt{1-k^2\sin^2\varphi}}\right] - \tan^{-1}\left[\frac{(q-k^2)\sin\varphi\cos\varphi}{A_{qk}\sqrt{1-k^2\sin^2\varphi}}\right]\right\}, \tag{B 4}$$

where in (B 3) we have $\cot\psi = k'\tan\varphi$ and in (B 4) n is as given in (A 13). Using (A 21) and (B 1)–(B 4) we can, after a lengthy algebra, establish the relation

$$G(\varphi,n,k) + G(\psi,k^2/q,k) = \frac{1}{2} - \frac{\pi}{2K}[F(\varphi,k) - F(\psi,k)]. \tag{B 5}$$

From this last equation (and the similar expression with m and p replacing n and q, respectively), we obtain the identity

$$H(\varphi,m,n,k) = H(\psi,k^2/q,k^2/p,k), \tag{B 6}$$

with m and n given by (A 13) and $\cot\psi = k'\tan\varphi$. This is precisely the relation (3.24) if we identify $m = u$, $n = v$, $r = k^2/q$ and $t = k^2/p$.

REFERENCES

Baker, G., Siegel, M., & Tanveer, S. 1995 A well-posed numerical method to track isolated conformal-map singularities in Hele-Shaw flow. *J. Comput. Phys.* **120**, 348–364.

Ben Amar, M. 1991*a* Viscous fingering in a wedge. *Phys. Rev.* A **44**, 3673–3685.

Ben Amar, M. 1991*b* Exact self-similar shapes in viscous fingering. *Phys. Rev.* A **44**, 5724–5727.

Brener, E., Levine, H. & Tu, Y. H. 1991 Nonsymmetric Saffman–Taylor fingers. *Phys. Fluids* A **3**, 529–534.

Burgess, D. & Tanveer, S. 1991 Infinite stream of Hele-Shaw bubbles. *Phys. Fluids* A **3**, 367–379.

Byrd, P. F. & Friedman, M. D. 1971 *Handbook of Elliptic Integrals for Engineers and Scientists.* Springer.

Carrier, G. F., Krook, M. & Pearson, C. 1983 *Functions of a Complex Variable.* Hod Books.

Combescot, R. & Dombre, T. 1989 Selection in the anomalous Saffman–Taylor fingers induced by a bubble. *Phys. Rev.* A **39**, 3525–3535.

Couder, Y., Gérard, N. & Rabaud, M. 1986 Narrow fingers in the Saffman–Taylor instability. *Phys. Rev.* A **34**, 5175–5178.

Dawson, S. P. & Mineev-Weinstein, M. 1994 Long-time behavior of the *n*-finger solution of the Laplacian growth equation. *Physica* D **73**, 373–387.

Hong, D. C. & Family, F. 1988 Bubbles in the Hele-Shaw cell: Pattern selection and tip perturbation. *Phys. Rev.* A **38**, 5253–5259.

Hong, D. C. & Langer, J. S. 1987 Pattern selection and tip perturbations in the Saffman–Taylor problem. *Phys. Rev.* A **36**, 2325–2332.

Howison, S. D. 1992 Complex variable methods in Hele–Shaw moving boundary problems. *Eur. J. Appl. Maths* **3**, 209–224.

Ikeda, E. & Maxworthy, T. 1990 Experimental study of the effect of a small bubble at the nose of a larger bubble in a Hele-Shaw cell. *Phys. Rev.* A **41**, 4367–4370.

Kessler, D., Koplik, J. & Levine, H. 1988 Pattern selection in fingered growth phenomena. *Adv. Phys.* **37**, 255–339.

Magdaleno, F. X. & Casademunt, J. 1998 Two-finger selection theory in the Saffman–Taylor problem. *Phys. Rev.* E **60**, R5013–R5016.

Maxworthy, T. 1986 Bubble formation, motion and interaction in a Hele-Shaw cell. *J. Fluid Mech.* **173**, 95–114.

Millar, R. F. 1992 Bubble motion along a channel in a Hele-Shaw cell: A Schwarz function approach. *Complex Variables* **18**, 13–25.

Mineev-Weinstein, M. B. 1998 Selection of the Saffman–Taylor finger width in the absence of surface tension: an exact result. *Phys. Rev. Lett.* **80**, 2113–2116.

Pelcé, P. 1988 *Dynamics of Curved Fronts.* Academic.

Rabaud, M., Couder, Y. & Gérard, N. 1988 Dynamics and stability of anomalous Saffman–Taylor fingers. *Phys. Rev.* A **37**, 935–947.

Saffman, P. G. 1959 Exact solutions for the growth of fingers from a flat interface between two fluids in a porous medium or Hele-Shaw cell. *Q. J. Mech. Appl. Maths* **12**, 146–150.

Saffman, P. G. & Taylor G. I. 1958 The penetration of a fluid into a porous medium or Hele-Shaw cell containing a more viscous liquid. *Proc. R. Soc. Lond.* A **245**, 312–320.

Tanveer, S. 1986 The effect of surface tension on the shape of a Hele-Shaw cell bubble. *Phys. Fluids* **29**, 3537–3548.

Tanveer, S. 1987 New solutions for steady bubbles in a Hele-Shaw cell. *Phys. Fluids* **30**, 651–658.

Tanveer, S. 1992 Viscous displacement in a Hele-Shaw cell. In *Asymptotics beyond All Orders* (ed. H. Segur, S. Tanveer & H. Levine), pp. 131–153. Plenum.

Taylor, G. I. & Saffman, P. G. 1959 A note on the motion of bubbles in a Hele-Shaw cell and porous medium. *Q. J. Mech. Appl. Maths* **12**, 265–279.

Tian, F. R. & Vasconcelos, G. L. 1993 Rotation invariance for steady Hele-Shaw flows. *Phys. Fluids* A **5**, 1863–1865.

Vasconcelos, G. L. 1993*a* Exact-solutions for a stream of bubbles in a Hele-Shaw cell. *Proc. R. Soc. Lond.* A **442**, 463–468.

Vasconcelos, G. L. 1993*b* Exact solutions for Hele-Shaw flows with surface tension: The Schwarz-function approach. *Phys. Rev.* E **48**, R658–R660.

Vasconcelos, G. L. 1994 Multiple bubbles in a Hele-Shaw cell. *Phys. Rev.* E **50**, R3306–R3309.

Vasconcelos, G. L. 1998 Exact solutions for N steady fingers in a Hele-Shaw cell. *Phys. Rev.* E **58**, 6858–6860.

Vasconcelos, G. L. 1999 Motion of a finger with bubbles in a Hele-Shaw cell. *Phys. Fluids* **11**, 1281–1283.

Vasconcelos, G. L. 2000 Analytic solution for two bubbles in a Hele-Shaw cell. *Phys. Rev.* E **62**, R3047–R3049.

Vasconcelos, G. L. 2001 Comment on 'Two-finger selection theory in the Saffman–Taylor problem.' *Phys. Rev.* E **63**, 043101-1–043101-2.

Vasconcelos, G. L. & Kadanoff, L. P. 1991 Stationary solutions for the Saffman–Taylor problem with surface tension. *Phys. Rev.* A **44**, 6490–6495.